

The BER Performance of the LDPC-Coded MPPM over Turbulence UWOC Channels

Jiang, Hongyan; He, Ning; Popoola, Wasiu; Rajbhandari, Sujan

Photonics

Published: 16/05/2022

Publisher's PDF, also known as Version of record

[Cyswllt i'r cyhoeddiad / Link to publication](#)

Dyfyniad o'r fersiwn a gyhoeddwyd / Citation for published version (APA):

Jiang, H., He, N., Popoola, W., & Rajbhandari, S. (2022). The BER Performance of the LDPC-Coded MPPM over Turbulence UWOC Channels. *Photonics*, 9(5).

Hawliau Cyffredinol / General rights

Copyright and moral rights for the publications made accessible in the public portal are retained by the authors and/or other copyright owners and it is a condition of accessing publications that users recognise and abide by the legal requirements associated with these rights.

- Users may download and print one copy of any publication from the public portal for the purpose of private study or research.
- You may not further distribute the material or use it for any profit-making activity or commercial gain
- You may freely distribute the URL identifying the publication in the public portal ?

Take down policy

If you believe that this document breaches copyright please contact us providing details, and we will remove access to the work immediately and investigate your claim.

The BER Performance of the LDPC-Coded MPPM over Turbulence UWOC Channels

Rajbhandari, Sujan

Photonics

Published: 16/05/2022

Publisher's PDF, also known as Version of record

[Cyswllt i'r cyhoeddiad / Link to publication](#)

Dyfyniad o'r fersiwn a gyhoeddwyd / Citation for published version (APA):
Rajbhandari, S. (2022). The BER Performance of the LDPC-Coded MPPM over Turbulence UWOC Channels. *Photonics*, 9(5).

Hawliau Cyffredinol / General rights

Copyright and moral rights for the publications made accessible in the public portal are retained by the authors and/or other copyright owners and it is a condition of accessing publications that users recognise and abide by the legal requirements associated with these rights.


- Users may download and print one copy of any publication from the public portal for the purpose of private study or research.
- You may not further distribute the material or use it for any profit-making activity or commercial gain
- You may freely distribute the URL identifying the publication in the public portal ?

Take down policy

If you believe that this document breaches copyright please contact us providing details, and we will remove access to the work immediately and investigate your claim.

Article

The BER Performance of the LDPC-Coded MPPM over Turbulence UWOC Channels

Hongyan Jiang ^{1,2}, Ning He ^{1,2}, Xin Liao ^{1,2}, Wasiu Popoola ³  and Sujan Rajbhandari ^{4,*}

¹ School of Information and Communication, Guilin University of Electronic Technology, Guilin 541004, China; jianghy@guet.edu.cn (H.J.); eicnhe@guet.edu.cn (N.H.); liaoshin@guet.edu.cn (X.L.)

² Guangxi Key Laboratory of Wireless Broadband Communication and Signal Processing, Guilin 541004, China

³ Institute for Digital Communications, School of Engineering, The University of Edinburgh, Edinburgh EH9 3FD, UK; w.popoola@ed.ac.uk

⁴ DSP Centre of Excellence, School of Computer Science and Electronic Engineering, Bangor University, Bangor LL57 1UT, UK

* Correspondence: s.rajbhandari@bangor.ac.uk

Abstract: Turbulence-induced fading is a critical performance degrading factor for underwater wireless optical communication (UWOC) systems. In this paper, we propose a quasi-cyclic (QC) low-density parity-check (LDPC) code with multiple-pulse-position modulation (MPPM) to overcome turbulence-induced fading. MPPM is adopted as a compromise between the low-power efficiency of on-off keying (OOK) and the low bandwidth efficiency of pulse position modulation (PPM). The bit error rate (BER) performance of LDPC-coded MPPM over turbulence UWOC channels is investigated. The log-likelihood ratio (LLR) of MPPM is derived, and a simplified approximation is used for iterative decoding. Subsequently, the closed-form expression of the BER, without forward error correction (FEC) code, is obtained for the generalized-gamma (GG) fading model. Finally, Monte-Carlo (MC) simulation results are provided to demonstrate the correctness of the derived closed-form expressions and the effectiveness of the LDPC code with simplified LLR to improve the BER performance for different MPPM formats over fading channels.

Keywords: UWOC; LDPC; MPPM; BER; fading



Citation: Jiang, H.; He, N.; Liao, X.; Popoola, W.; Rajbhandari, S. The BER Performance of the LDPC-Coded MPPM over Turbulence UWOC Channels. *Photonics* **2022**, *9*, 349. <https://doi.org/10.3390/photonics9050349>

Received: 10 April 2022

Accepted: 13 May 2022

Published: 16 May 2022

Publisher's Note: MDPI stays neutral with regard to jurisdictional claims in published maps and institutional affiliations.



Copyright: © 2022 by the authors. Licensee MDPI, Basel, Switzerland. This article is an open access article distributed under the terms and conditions of the Creative Commons Attribution (CC BY) license (<https://creativecommons.org/licenses/by/4.0/>).

1. Introduction

The fifth-generation (5G) wireless communication network is widely deployed, which has significantly increased capacity and supported larger-scale connections, but is limited primarily to terrestrial communication. The upcoming sixth-generation (6G) network is expected to provide wider coverage with a seamless connection from space to underwater [1]. Though an important part of heterogeneous and massive-scale networks, underwater wireless communication has many challenges, due to the complex nature of the underwater channel. Underwater wireless optical communication (UWOC) is considered an effective solution, due to its high energy-efficiency, high-speed communication and security [2]. To make the UWOC robust and reliable in all conditions, the effects of absorption, scattering and turbulence, resulting in attenuation, delay spread and fading must be comprehensively understood. Many studies have experimentally and theoretically characterized the underwater optical absorption and scattering caused by suspended matter, ions, plankton and other factors [3–5]. Random fluctuations of water density, temperature and salinity, resulting from surf, tide geothermal and so on, generate random variations on the refractive index of water, which causes turbulence. When a light beam passes through water, turbulence effects, such as beam wandering, spreading, jitter, and intensity fluctuation (i.e., fading), degrade the received optical signal [6,7]. It is of great significance to investigate the fading characteristics of underwater turbulence and to find corresponding mitigation techniques.

Various studies have investigated the scintillation index, describing turbulence strength, which is affected by the eddy diffusivity ratio, aperture diameter, wave model and so

on [8–10]. Experimental studies also characterized underwater turbulence caused by different phenomena and proposed statistical distributions to fit the optical intensity fluctuations [7,11–16]. A combination of exponential and log-normal distributions was proposed in [11] to describe the fluctuations of the probability density function (PDF) in the presence of air bubbles. Furthermore, to obtain closed-form and analytically tractable expressions for crucial system performance metrics, the mixture exponential-gamma distribution is adopted to characterize channel irradiance fluctuations resulting from air bubbles [12]. In [13,14], a generalized-gamma (GG) distribution was used to model the fading of coherent and non-coherent light induced by temperature inhomogeneity. For salinity variation induced turbulence, Weibull distribution can efficiently fit the acquired scintillation data [15]. Moreover, the mixture exponential-GG (EGG) distribution can describe the statistics of underwater optical beam irradiance fluctuations due to air bubbles and temperature gradient [16]. Experimental study under different underwater scenarios, incorporating the effects of temperature gradients, salinity variation and air bubbles, demonstrate that using beam expander-and-collimator (BEC) at the transmitter side, and/or aperture averaging lens (AAL) at the receiver side, GG and exponentiated Weibull (EW) distributions can excellently match the PDF of measured data in weak to strong turbulence [7].

Several turbulence mitigation techniques, such as channel coding [17], multi-hop relaying transmission [18], aperture averaging [19], and spatial diversity [20], were studied. Spatial diversity with linear combining at the receiver, such as equal gain combining (EGC) and maximum ratio combining (MRC), can effectively alleviate fading impairments. Though the MRC has optimal linear diversity reception, it is complicated due to the requirements of both phase and fading amplitude estimation of all branches. However, EGC, with low complexity and implementation simplicity, performs close to MRC in most scenarios [21]. Aperture averaging can reduce the scintillation by enlarging the receiver aperture area. System size and cost increase as aperture area increases, while performance gain saturates due to background noise. The channel coding technique can substantially reduce the error rate in weak turbulence channels. However, it should be combined with other techniques to combat the degrading effects in moderate to strong turbulence [22].

UWOC performance also greatly depends on the modulation scheme. Modulation schemes are based on spectral efficiency, power efficiency and implementation complexity. Due to implementation simplicity, UWOC usually employs intensity modulation with direct detection (IM/DD), rather than a coherent technique. Subcarrier intensity modulation (SIM), such as phase-shift keying (PSK) and quadrature amplitude modulation (QAM), can effectively exploit bandwidth and improve error performance, but has issues, such as clipping requirements, limited modulation index, and susceptibility to nonlinearity [23]. Furthermore, to overcome adverse effects of strong turbulence on the performance of QAM/PSK, adaptive modulation and diversity/coding are required [24–26]. On-off keying (OOK) and pulse position modulation (PPM) schemes are widely used in optical communication because of their simplicity. OOK format has superior bandwidth efficiency, but inferior average power efficiency compared with PPM. Additionally, the OOK scheme requires an adaptive threshold to achieve optimal detection in turbulent channels. To overcome these drawbacks, power-efficient multipulse PPM (MPPM) can be adopted as a tradeoff between OOK and PPM. The MPPM scheme has higher power efficiency compared to OOK and higher bandwidth efficiency compared to the PPM [27]. Optical sources can be efficiently driven with a large current for pulse modulation, ensuring a relatively high signal-to-noise ratio (SNR) [28].

Several works reported the performance of the MPPM-based free-space optical (FSO) and UWOC systems over turbulent channels. The study in [29] presented the performance of PPM and MPPM formats in conjunction with a binary convolutional code and iterative soft-decision detection for the FSO communication with weak turbulence modeled by a log-normal distribution. The influence of bit-symbol mapping of MPPM on the iterative receiver performance was analyzed and then provided a design rule to obtain optimal mappings for the iterative detection scheme. The symbol error rate (SER) performance of MPPM-based

FSO system with fixed decision threshold (FDT), optimized decision threshold (ODT) and dynamic decision threshold (DDT) over EW-distributed fading channels were studied in [30]. The study derived closed-form SER expressions for the three thresholds scheme and investigated the effects of aperture averaging. It was shown that the performance of DDT is better than those of FDT and ODT. However, the DDT scheme is computationally complex due to requirements for channel state information (CSI).

Furthermore, combining effects of EW-distributed fading and pointing errors, SER performance of (m, n) MPPM-based FSO system with a new soft decoder is studied in [31]. The decoder considers the largest m slots of a received signal block (n slots) as the signal slots without CSI. The new soft-decision technique outperforms the DDT scheme. In [32], comprehensive theoretical SER expressions (not closed-form) for soft-decision MPPM, without CSI, and simplified expressions for fast and slow fading for the FSO non-memoryless channels were derived. The numerical and simulation results for log-normal and gamma-gamma fading were presented. Taking into account the effects of inter-symbol interference, oceanic turbulence and receiver noise, the BER performance of spatial diversity with MPPM receivers applied to UWOC systems operating over log-normal turbulence was investigated in [33]. For the UWOC systems affected by salinity turbulence, the BER of variable weight MPPM coding schemes was evaluated, based on Weibull distribution in [34]. In [31,34], curve-fitting methods were used to obtain high accuracy conditional SER and BER formulas in the additive white Gaussian noise (AWGN) channel, and the corresponding closed-form SER and BER expressions in the presence of turbulence were derived, based on Gauss-Laguerre integration and the cumulative distribution function (CDF) of the transmitted optical irradiance.

This paper analyses the BER performance of low-density parity-check (LDPC)-coded MPPM UWOC systems with aperture averaging over turbulence channels. To the best of our knowledge, there is no detailed BER performance evaluation of LDPC-coded MPPM UWOC systems over turbulence channels with different fading models. LDPC is a powerful coding scheme with a sparse parity check matrix [35], which can approach the Shannon capacity in the AWGN channel. The LDPC code outperforms Turbo and Reed–Solomon (RS) codes in bursty-error channels and can be very effective for high-speed optical systems because of its low hardware complexity and low latency [36,37]. In this work, Quasi-Cyclic (QC) LDPC codes described in IEEE.802.16 standard [38] are investigated due to their pros, such as simple construction, easy hardware implementation, lower computational complexity of the encoding and decoding, and flexible adjustment of the code length and the code rate [39]. GG and EW distributions are adopted in the study as aperture averaging alleviates intensity scintillation and makes GG and EW distribution suitable for modelling fading in all the considered turbulent scenarios, as outlined in [7]. The main contributions of this paper are as follows: (i) the initial log-likelihood ratio (LLR) for LDPC decoding is derived, based on Gaussian distribution and Jacobian logarithm, and then simplified (ii) based on Gauss-Laguerre integration and the CDF of GG distribution, the closed-form expression of the BER without LDPC, but experiencing GG fading, is presented, and (iii) Monte-Carlo (MC) simulation is used to verify the derived BER expressions and the efficiency and applicability of the LDPC scheme to mitigate turbulence-induced fading.

The remainder of this paper is organized as follows: Section 2 describes the LDPC-coded MPPM UWOC system, channel model and general assumptions. The soft demapping and decoding are detailed in Section 3. For comparison, the BER performance without LDPC code over the GG fading channel is analyzed in Section 4. Numerical and simulation results are presented, compared and discussed in Section 5. Finally, Section 6 concludes the paper.

2. System and Channel Models

Figure 1 shows a simplified configuration of an LDPC-coded MPPM UWOC system over turbulent channels. At the transmitter, pseudorandom binary streams are parsed into groups of k -bits and encoded by a QC-LDPC encoder following IEEE.802.16 standard,

generating corresponding groups of codewords with m -bits, where k and m are the information length and code length of LDPC, respectively. Further, the codewords are grouped into blocks with a length of L , and then the blocks are mapped into symbol constellations on the basis of w -pulse M -slot (M, w) MPPM format, producing a modulated electrical signal, where $L = \lfloor \log_2 \left(\frac{M}{w} \right) \rfloor$. Assuming no interslot interference and perfect slot synchronization, the system performance is not affected by the bit-to-symbol mapping. The electrical signal modulates the laser, resulting in an optical signal x with an average optical power of P_{av} . After propagating through the turbulent underwater channel, the optical signal is received and converted to an electrical signal y by a photodetector (PD). Subsequently, the signal is demodulated, based on soft-decision with log-likelihood ratio information, which is further fed to the decoder for iterative decoding.

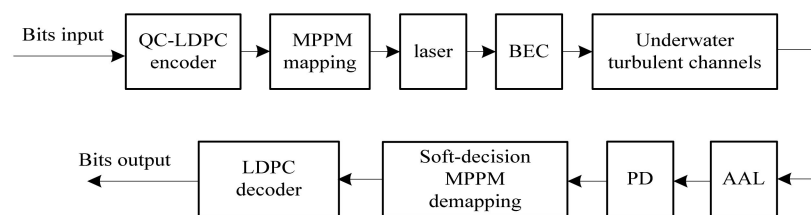


Figure 1. Schematic of the LDPC-coded MPPM UWOC system over turbulent channels.

The received electrical signal is expressed as [31]:

$$y = Rhx + n, \quad (1)$$

where R is the photodetector responsivity, x is equal to zero and MP_{av}/w in the non-signal time slot and signal time slot, respectively. The AWGN with zero mean is represented by n , single-sided power spectral density by N_0 , and the variance of $\sigma_n^2 = N_0/2$. The channel gain is h , which can be expressed as $h = h_l h_f$, where h_l is the path loss and is assumed to be unity, h_f represents the slow-fading coefficient. Here, we use GG distribution to model received optical intensity fluctuation.

The PDF of GG distribution is expressed as [7]:

$$f_{GG}(s) = \frac{p}{a^d \Gamma(d/p)} s^{d-1} \exp(-(s/a)^p), \quad s > 0 \quad (2)$$

where d , a and p are fading, scaling and shape parameters, respectively. The gamma function is represented by $\Gamma(\cdot)$. The fading coefficient is described as $h_f \sim GG(m, v, \Omega)$, the CDF of which is given by:

$$F_{GG}(s) = \frac{\Upsilon\left(\frac{d}{p}, \left(\frac{s}{a}\right)^p\right)}{\Gamma(d/p)}, \quad (3)$$

where $\Upsilon(a, x)$ denotes the lower incomplete gamma function.

At the receiver, slot-by-slot detection is applied. Thus, the received electrical signal in one slot can be written as:

$$y = \begin{cases} Rh_l h_f MP_{av}/w + n & \text{signal timeslot} \\ n & \text{non-signal timeslot} \end{cases} \quad (4)$$

Further, the instantaneous electrical signal-to-noise ratio (SNR) is given by:

$$\gamma = \left(\frac{Rh_l MP_{av}}{\sqrt{2}w\sigma_n} \right)^2 h_f^2 = \bar{\gamma} h_f^2 \quad (5)$$

where $\bar{\gamma} = \left(\frac{Rh_1 MP_{av}}{\sqrt{2w\sigma_n}} \right)^2$ represents the average SNR in the absence of fading.

3. LLR Calculation

The min-sum algorithm is adopted for iterative decoding due to a lower-complexity approximation to the sum-product algorithm (SPA) [40]. Prior to decoding, the initial LLR of every bit is obtained from soft de-mapping. Let $\mathbf{S} = [\mathbf{S}_1, \mathbf{S}_2, \dots, \mathbf{S}_q]$ be the set of all possible (M, w) MPPM, where $q = \binom{M}{w}$, $\mathbf{S}_i = [s_1, s_2, \dots, s_M]$ is a vector denoting a slot-symbol for the (M, w) MPPM format with w pulses and M slots. $\mathbf{C} = \{\mathbf{C}_1, \mathbf{C}_2, \dots, \mathbf{C}_{2^L}\} \in \mathbf{S}$ is the set of effective symbols. Assuming the bit-symbol $\mathbf{A}_i = [a_1, a_2, \dots, a_L]$ is mapped into the slot-symbol $\mathbf{C}_i = [c_1, c_2, \dots, c_M]$, its corresponding received slot-symbol is expressed as $\mathbf{Y}_i = [y_1, y_2, \dots, y_M]$. Let \mathbf{H}_i denote the set of indices for which \mathbf{C}_i has a signal time slot. Let $P_s(y)$ and $P_n(y)$ be the conditional probability density functions of a received slot with a value of y on signal and non-signal time slots. The likelihood ratio of a slot of y is given by $lr(y) = P_s(y)/P_n(y)$ [41]. Based on the previous assumption, we derive the bit LLR as follows.

The probability of the l -th bit in one symbol conditioned on \mathbf{Y} is given by:

$$P(a_l = b|\mathbf{Y}) = \sum_{\substack{\mathbf{C}_i \in \mathbf{C} \\ a_l = b}} P(\mathbf{C}_i|\mathbf{Y}), \quad i \in \{1, 2, \dots, 2^L\}, b \in \{0, 1\}. \quad (6)$$

Using Bayes theorem, we have:

$$P(\mathbf{C}_i|\mathbf{Y}) = \frac{P(\mathbf{Y}|\mathbf{C}_i)P(\mathbf{C}_i)}{P(\mathbf{Y}_i)} = \frac{P(\mathbf{Y}|\mathbf{C}_i)P(\mathbf{C}_i)}{\sum_{j=1}^{2^L} P(\mathbf{Y}|\mathbf{C}_j)P(\mathbf{C}_j)}. \quad (7)$$

It is assumed that the transmitted symbols \mathbf{C}_i are equiprobable, i.e., the priori $P(\mathbf{C}_i)$ remains the same, resulting in [42]:

$$P(\mathbf{C}_i|\mathbf{Y}) = \frac{P(\mathbf{Y}|\mathbf{C}_i)}{\sum_{j=1}^{2^L} P(\mathbf{Y}|\mathbf{C}_j)}; \quad (8)$$

where:

$$P(\mathbf{Y}|\mathbf{C}_i) = \prod_{e \in \mathbf{H}_i} P_s(y_e) \prod_{z \notin \mathbf{H}_i} P_n(y_z) = \prod_{e \in \mathbf{H}_i} \frac{P_s(y_e)}{P_n(y_e)} \prod_{z=1}^M P_n(y_z) = \prod_{e \in \mathbf{H}_i} lr_e \prod_{z=1}^M P_n(y_z). \quad (9)$$

Substituting (9) into (8), we obtain:

$$P(\mathbf{C}_i|\mathbf{Y}) = \frac{\prod_{e \in \mathbf{H}_i} lr_e \prod_{z=1}^M P_n(y_z)}{\sum_{j=1}^{2^L} \left[\prod_{e \in \mathbf{H}_j} lr_e \prod_{z=1}^M P_n(y_z) \right]} = \frac{\prod_{e \in \mathbf{H}_i} lr_e}{\sum_{j=1}^{2^L} \prod_{e \in \mathbf{H}_j} lr_e}. \quad (10)$$

Using (10) and (6), we have:

$$P(a_l = b|\mathbf{Y}) = \frac{\sum_{\substack{\mathbf{C}_i \in \mathbf{C} \\ a_l = b}} \prod_{e \in \mathbf{H}_i} lr_e}{\sum_{j=1}^{2^L} \prod_{e \in \mathbf{H}_j} lr_e}. \quad (11)$$

So, the LLR of a_l is expressed as:

$$L(a_l) = \ln \left[\frac{P(a_l = 0|Y)}{P(a_l = 1|Y)} \right] = \ln \left(\sum_{\substack{\mathbf{C}_i \in \mathbf{C} \\ a_l = 0}} \prod_{e \in H_i} l r_e \right) - \ln \left(\sum_{\substack{\mathbf{C}_i \in \mathbf{C} \\ a_l = 1}} \prod_{e \in H_i} l r_e \right); \quad (12)$$

$L(a_l)$ is the initial LLR for further iterative decoding of LDPC. When the MPPM system is without LDPC, the bit a_l can be directly decoded based on the following decision:

$$a_l = \begin{cases} 1, & L(a_l) < 0 \\ 0, & L(a_l) > 0 \end{cases} \quad (13)$$

According to (1), $P_s(y)$ should be the convolution of PDFs of channel gain and AWGN. However, to simplify the calculation, herein we approximate $P_s(y)$ with Gaussian distribution due to slow fading. Thus, we obtain:

$$l r(y) = \frac{P_s(y)}{P_n(y)} = \exp \left(\frac{2yI - I^2}{N_0} \right) \quad (14)$$

where $I = RhMP_{av}/w$. Substituting (14) into (12), we have:

$$L(a_l) = \ln \left[\sum_{\substack{\mathbf{C}_i \in \mathbf{C} \\ a_l = 0}} \exp \left(\sum_{e \in H_i} \frac{2y_e I - I^2}{N_0} \right) \right] - \ln \left[\sum_{\substack{\mathbf{C}_i \in \mathbf{C} \\ a_l = 1}} \exp \left(\sum_{e \in H_i} \frac{2y_e I - I^2}{N_0} \right) \right] \quad (15)$$

The calculation of (15) is very difficult for a practical system because of the complex operation (even appearing infinity) and requirement of CSI. Thus, a simple and low computational complexity expression should be applied. Based on the approximation of $\ln(e^m + e^n) \approx \max(m, n)$ (Jacobian logarithm), (15) can be written as:

$$L(a_l) = \max_{\substack{\mathbf{C}_i \in \mathbf{C} \\ a_l = 0}} \left(\sum_{e \in H_i} \frac{2y_e I - I^2}{N_0} \right) - \max_{\substack{\mathbf{C}_i \in \mathbf{C} \\ a_l = 1}} \left(\sum_{e \in H_i} \frac{2y_e I - I^2}{N_0} \right) \quad (16)$$

Furthermore, it can be simplified to:

$$L(a_l) = \max_{\substack{\mathbf{C}_i \in \mathbf{C} \\ a_l = 0}} \left(\sum_{e \in H_i} y_e \right) - \max_{\substack{\mathbf{C}_i \in \mathbf{C} \\ a_l = 1}} \left(\sum_{e \in H_i} y_e \right) \quad (17)$$

In the simplification from (16) to (17), the absolute value of LLR is changed while its sign (plus or minus), which depends on the largest received slots and decides the bit, keeps the same due to monotonicity. Therefore, the simplification satisfies the requirement of the iterative soft decision but does not need CSI.

4. BER Performance without the FEC

To verify the efficiency of LDPC code to mitigate turbulence-induced fading, we compare the BERs with and without LDPC code in Section 5, prior to which approximated average BER of the MPPM UWOC system without FEC over GG-distributed fading channels are deduced.

The average BER P_b is obtained by averaging the conditional BER $p(\varepsilon|\gamma)$ over the fading channels as:

$$P_b = \int_0^\infty p(\varepsilon|\gamma)p_\gamma(\gamma)d\gamma \quad (18)$$

where $p_\gamma(\gamma)$ is the PDF of instantaneous SNR, and its CDF $F_\gamma(\gamma)$ can be obtained using (3) and (5), and is given as

$$F_\gamma(\gamma) = \frac{\Upsilon\left(\frac{d}{p}, \left(\frac{\gamma}{a^2\gamma}\right)^{p/2}\right)}{\Gamma(d/p)}. \quad (19)$$

A curve-fitting method is an alternative to derive the exact analytical expression of the conditional BER of MPPM-based systems [34,43]. A hyper-exponential fitting technique is applied to derive the closed-form approximation expression of the conditional BER in [34]. An exponential fitting, which is a special case of hyper-exponential fitting, is adopted to obtain the tractable closed-form conditional SER expression in [31]. Here, the hyper-exponential fitting is used, and thus we assume $p(\varepsilon|\gamma) = b_1 \exp(-b_2\gamma^{b_3})$, where b_1 , b_2 and $b_3 \in \mathbb{R}^+$ and are evaluated by fitting to the Monte Carlo-simulated BER in the absence of any fading (i.e., AWGN channel). The Monte Carlo simulation is verified to ensure the correctness prior to fitting, which is presented in Section 5. Then, with the integration by parts, change of variables and Gauss-Laguerre quadrature formulation [43], we have:

$$\begin{aligned} P_b &= - \int_0^\infty F_\gamma(\gamma)dp(\varepsilon|\gamma) \\ &= b_1 \sum_{i=1}^m w_i \frac{\Upsilon\left(\frac{d}{p}, \left[\frac{1}{a^2\gamma} \left(\frac{x_i}{b_2}\right)^{\frac{1}{b_3}}\right]^{p/2}\right)}{\Gamma(d/p)}; \end{aligned} \quad (20)$$

where x_i is the i th zero of Laguerre polynomials $L_m^\beta(x)$, $w_i = \Gamma(m + \beta + 1)x_i / \left\{ m! \left[(m + 1)L_{m+1}^\beta(x_i) \right]^2 \right\}$ is the corresponding weight coefficient and $\beta = 0$. $m = 10$ is assumed, and then values of x_i and w_i in (20) are shown in Table 1.

Table 1. Zeros of $L_{10}(x)$ and corresponding weight coefficients.

x_i	w_i
0.13779347054049237	0.308441
0.7294545495031706	0.40112
1.8083429017403165	0.218068
3.4014336978549595	0.0620875
5.552496140063418	0.00950152
8.330152746764144	0.000753008
11.843785837899944	0.0000282592
16.279257831377613	4.24931×10^{-7}
21.99658581198083	1.83956×10^{-9}
29.92069701227372	9.91183×10^{-13}

5. Results and Discussion

This section demonstrates the effect of LDPC code on alleviating turbulence-induced fading by comparing the BER performance of the coded and uncoded MPPM UWOC system in different fading scenarios modeled by various statistical distributions. An illustration of the system flowchart is given in Figure 2.

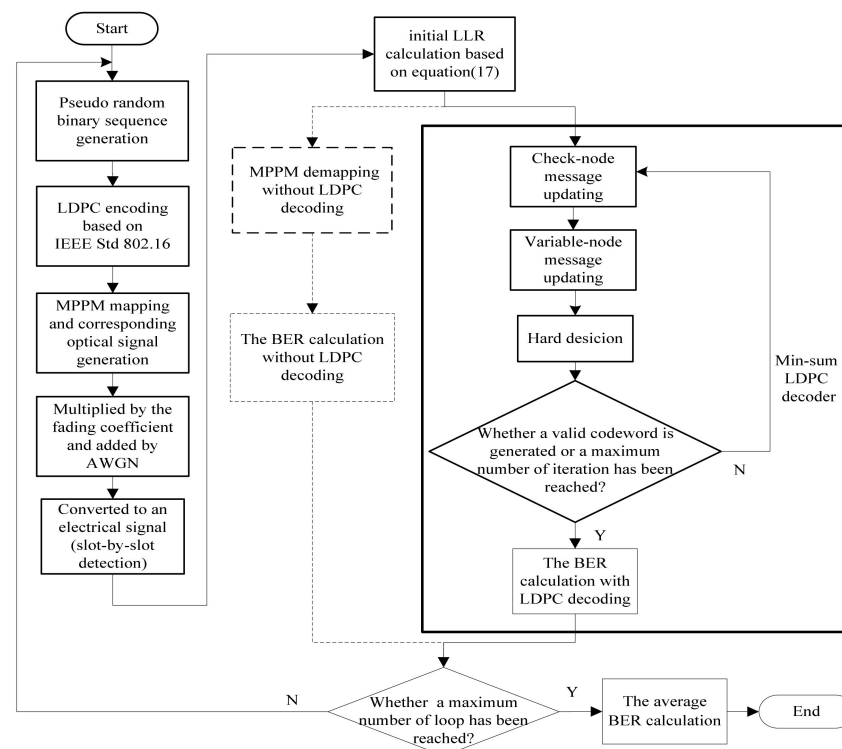


Figure 2. The flowchart for studying the effect of turbulence on UWOC using MPPM scheme.

Figure 3 shows the BER and SER of uncoded (5, 2) MPPM for the AWGN-only channel. The simulation results are utilized to obtain the constants b_1 , b_2 and b_3 of the conditional PDF $p(\epsilon|\gamma)$, which is verified by contrastive analysis. By comparison, the SER, based on the simplified LLRs of Equation (17) is close to, but lower than, that based on finding the largest slots as the symbol slot, i.e., $SER = 0.836 \exp(-0.5231\gamma)$, which is obtained using exponential fitting to the analytical SER in [31]. Meanwhile, the corresponding BER, based on simplified LLRs, is not greater than the BER upper bound defined in [27]. Hence, the correctness of the simulation for the system is demonstrated, resulting in $b_1 = 0.4251$, $b_2 = 0.5861$ and $b_3 = 0.9655$.

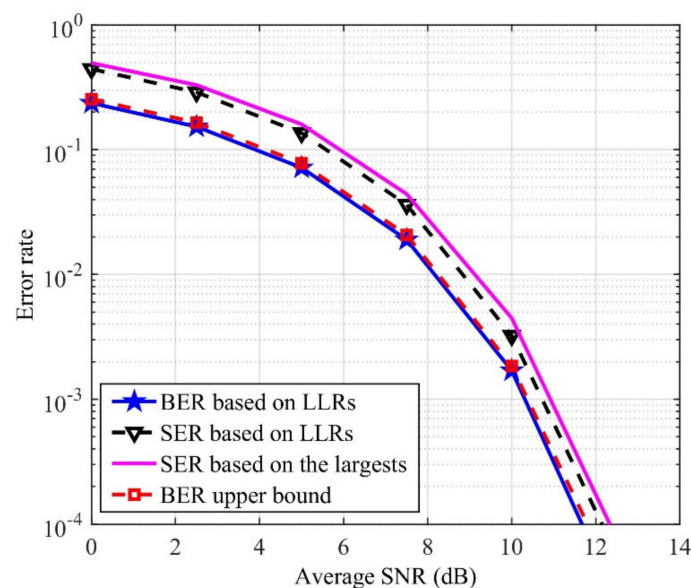


Figure 3. Bit error rate and symbol error rate of the (5, 2) MPPM UWOC system in the absence of fading.

Figure 4 shows the BER performance of the (5, 2) MPPM UWOC system in the presence of weak, moderate, and strong turbulences modeled by GG distribution. The channel parameters of GG distribution are obtained from [7] and given in Table 2, where aperture averaging was taken into account, as the experiments were carried out using AAL, and $\sigma_I^2 = \Gamma(d/p)\Gamma(\frac{d+2}{p})/\Gamma^2(\frac{d+1}{p}) - 1$ represents the scintillation index. The theoretical BERs without LDPC code are obtained using (20). As expected, the simulation and theoretical results demonstrate excellent matching, validating the mathematical analysis. The BERs increase with increase of the scintillation index σ_I^2 (i.e., turbulence strength). The LDPC code substantially improves the BER performance for all cases. For example, the LDPC coded system can achieve a BER of 10^{-5} at the SNRs of 14.4 dB and 19.9 dB, respectively, at moderate ($\sigma_I^2 = 0.5782$) and strong ($\sigma_I^2 = 2.0399$) turbulence. In the absence of the LDPC code, the BERs are higher than 10^{-2} at the SNR of 22 dB, demonstrating significant coding gain. In weak turbulence with $\sigma_I^2 = 0.2073$, a code gain of ~ 12.1 dB is obtained at the BER of 10^{-4} .

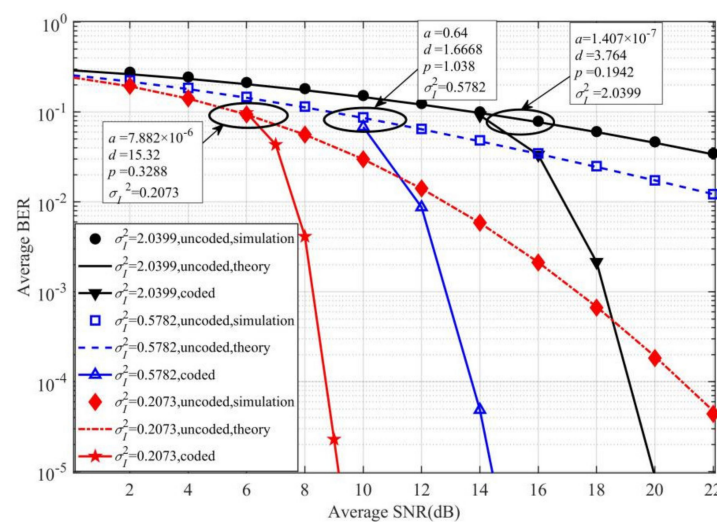


Figure 4. BERs of the (5, 2) MPPM UWOC system with/without LDPC code in the GG-distributed fading channel with different scintillation indexes.

Table 2. The parameters of GG-distributed fading channels, adopted from [7].

Channel Condition	a	d	p	σ_I^2
Salinity random variations	7.882×10^{-6}	15.32	0.3288	0.2073
Temperature random variations mixed presence of air bubbles	0.64	1.6668	1.038	0.5782
Random presence of air bubbles	1.407×10^{-7}	3.764	0.1942	2.0399

Figure 5 presents the BER performance of (6, 3) MPPM UWOC system over the same turbulence channel, but modeled by different popular statistical distributions, including log-normal, gamma-gamma, EW and GG. Log-normal and gamma-gamma generally model fading induced by weak and moderate/strong turbulence, respectively [44]. Here, the four distributions were used to fit the same experimental data suffering weak fading described in Table 2, Line 2 (the detailed parameters are given in [7], Table IV, Line 5). Uncoded UWOC system shows a similar BER performance at low SNRs irrespective of channel model. A difference in BER performance is observed at higher SNR. Log-normal distribution underestimates the fading, resulting in the best BER performance among the four-channel fading models. The LDPC code with simplified LLRs always improves the BER performance of MPPM for the UWOC systems and shows identical BER performance,

irrespective of turbulence-induced fading distribution. For the four distributions, coding gains are 10.7 dB, 12.4 dB, 13.6 dB and 11.8 dB at the BER of 10^{-4} , respectively.

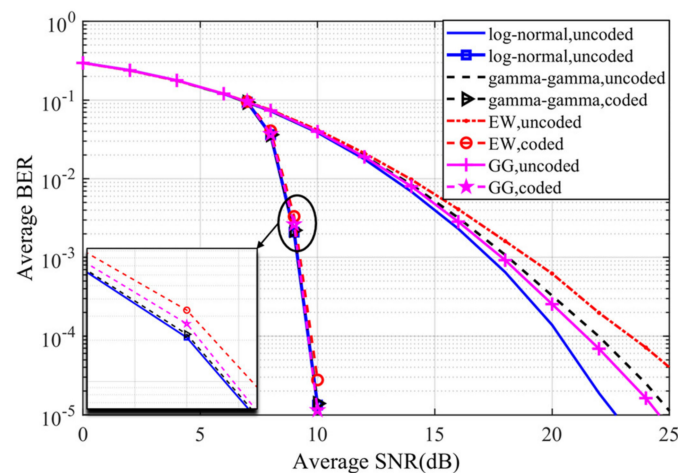


Figure 5. BERs of the (6, 3) MPPM UWOC system with/without LDPC code in the same weak turbulence channel modeled by different statistical distributions.

Figure 6 shows the comparison of BERs of uncoded and coded OOK, PPM and MPPM UWOC systems over a weak turbulence channel model by GG distribution. The initial LLR of OOK is given by $(2yI - I^2)/N_0$, where I is a constant corresponding to the fixed threshold value. PPM is a special case of (M, w) MPPM (i.e., $w = 1$), whose initial LLR is obtained by (17). As reported in other work, the uncoded OOK with a fixed threshold shows a high error floor in the turbulence channel [45]. An adaptive threshold, that depends on the turbulence strength, is required for optimum OOK performance. The LDPC coding significantly improves the OOK performance, but the performance of coded OOK is inferior to MPPM. That is because LDPC decoding depends on initial LLRs (i.e., the received signal, which is significantly deteriorated by turbulence). By comparison, (6, 3), (5, 2) and (4, 1) MPPM offer improved BER performance with coding gains of 11.8 dB, 12.1 dB and 12.3 dB at the BER of 10^{-4} , respectively. Though the BER performance improves and coding gains get higher for (6, 3), (5, 2) and (4, 1) MPPM, the spectral efficiencies given by $\eta = \lfloor \log_2 \left(\frac{M}{w} \right) \rfloor / M$ decrease accordingly. This is expected, as MPPM always has a tradeoff between spectral efficiency and power efficiency [27].

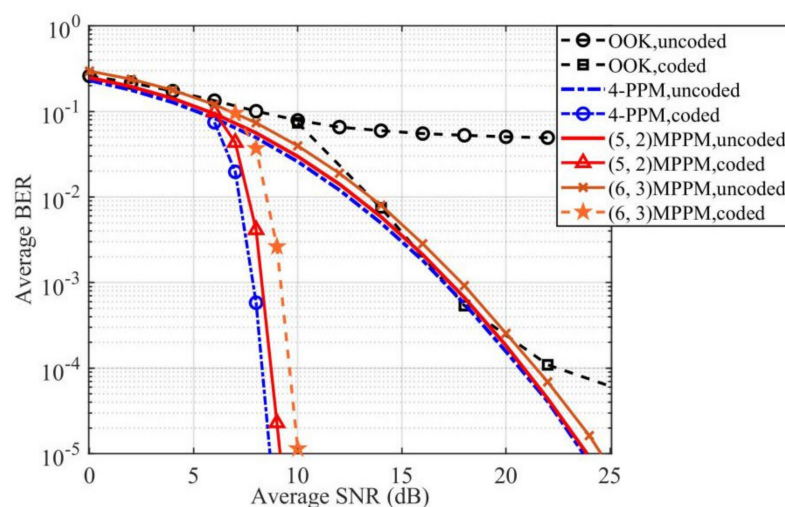


Figure 6. BERs of the UWOC systems with different modulation schemes in the GG fading channel with a scintillation index of $\sigma_I^2 = 0.2073$.

6. Conclusions

In this paper, we evaluated the BER performance of LDPC-coded MPPM UWOC systems over turbulence-induced fading channels. For iterative decoding, the initial bit LLR of MPPM was derived and simplified, based on Gaussian distribution and Jacobian logarithm. Furthermore, a closed-form expression of the BER without FEC was presented for using the Gauss-Laguerre integration and GG distribution fading models. MC simulation was adopted to verify the correctness of the closed-form analytical results and to demonstrate the effectiveness of LDPC code with simplified LLRs on turbulence mitigation for different modulation formats. LDPC code with simplified LLRs can significantly improve BER performance in fading channels. LDPC offered code gains of 11.8 dB, 12.1 dB and 12.3 dB at $\text{BER} = 10^{-4}$ for (6, 3), (5, 2) and (4, 1) MPPM scheme in the GG fading channel with a scintillation index of $\sigma_I^2 = 0.2073$. Furthermore, LDPC code with simplified LLRs is suitable for practical implementation because of less computational complexity and no requirement for CSI.

Author Contributions: Conceptualization, H.J. and S.R.; methodology, H.J. and S.R.; software, H.J. and S.R.; validation, H.J. and S.R.; investigation, H.J., S.R., N.H. and X.L.; writing—original draft preparation H.J. and S.R.; writing—review and editing, S.R. and W.P.; funding acquisition, N.H. and H.J. All authors have read and agreed to the published version of the manuscript.

Funding: This research was funded in part by the National Natural Science Foundation of China (grant number 61961008), and in part by the Dean Project of Guangxi Key Laboratory of Wireless Broadband Communication and Signal Processing (grant number GXKL06200127). S.R. works at the DSP Centre, which has been part-funded by the European Regional Development Fund through Welsh Government and also by the North Wales Growth Deal through Ambition North Wales, Welsh Government, and UK Government.

Conflicts of Interest: The authors declare no conflict of interest.

References

- Jiang, R.; Sun, C.; Zhang, L.; Tang, X.; Wang, H.; Zhang, A. Deep Learning Aided Signal Detection for SPAD-Based Underwater Optical Wireless Communications. *IEEE Access* **2020**, *8*, 20363–20374. [\[CrossRef\]](#)
- Lian, J.; Gao, Y.; Wu, P.; Lian, D. Orthogonal frequency division multiplexing techniques comparison for underwater optical wireless communication systems. *Sensors* **2019**, *19*, 160. [\[CrossRef\]](#) [\[PubMed\]](#)
- Loisel, H.H.; André, M. Light scattering and chlorophyll concentration in Case 1 waters: A re-examination. *Limnol. Oceanogr.* **1998**, *43*, 847–858. [\[CrossRef\]](#)
- Tang, S.; Dong, Y.; Zhang, X. Impulse Response Modeling for Underwater Wireless Optical Communication Links. *IEEE Trans. Commun.* **2013**, *62*, 226–234. [\[CrossRef\]](#)
- Miramirkhani, F.; Uysal, M. Visible Light Communication Channel Modeling for Underwater Environments with Blocking and Shadowing. *IEEE Access* **2017**, *6*, 1082–1090. [\[CrossRef\]](#)
- Saeed, N.; Celik, A.; Al-Naffouri, T.Y.; Alouini, M.S. Underwater optical wireless communications, networking, and localization: A survey. *Ad. Hoc. Netw.* **2019**, *94*, 101935. [\[CrossRef\]](#)
- Vahid Jamali, M.; Mirani, A.; Parsay, A.; Abolhassani, B.; Nabavi, P.; Chizari, A.; Khorramshahi, P.; Abdollahramezani, S.; Salehi, J.A. Statistical Studies of Fading in Underwater Wireless Optical Channels in the Presence of Air Bubble, Temperature, and Salinity Random Variations (Long Version). *IEEE Trans. Commun.* **2018**, *66*, 4706–4723.
- Yue, P.; Wu, M.; Yi, X.; Cui, Z.; Luan, X. Underwater optical communication performance under the influence of the eddy diffusivity ratio. *J. Opt. Soc. Am. A* **2018**, *36*, 32–37. [\[CrossRef\]](#)
- Xu, G.; Lai, J. Average capacity analysis of the underwater optical plane wave over anisotropic moderate-to-strong oceanic turbulence channels with the Málaga fading model. *Opt. Express* **2020**, *28*, 24056. [\[CrossRef\]](#)
- Ata, Y.; Baykal, Y. Scintillations of optical plane and spherical waves in underwater turbulence. *J. Opt. Soc. Am. A* **2014**, *31*, 1552–1556. [\[CrossRef\]](#)
- Jamali, M.V.; Khorramshahi, P.; Tashakori, A.; Chizari, A.; Shahsavari, S.; Abdollah Ramezani, S.; Fazelian, M.; Bahrani, S.; Salehi, J.A. Statistical distribution of intensity fluctuations for underwater wireless optical channels in the presence of air bubbles. In Proceedings of the 2016 Iran Workshop on Communication and Information Theory (IWCIT), Tehran, Iran, 3–4 May 2016; pp. 1–6. [\[CrossRef\]](#)
- Zedini, E.; Oubei, H.M.; Kammoun, A.; Hamdi, M.; Ooi, B.S.; Alouini, M.-S. A New Simple Model for Underwater Wireless Optical Channels in the Presence of Air Bubbles. In Proceedings of the GLOBECOM 2017—2017 IEEE Global Communications Conference, Singapore, 4–8 December 2017; pp. 1–6. [\[CrossRef\]](#)

13. Oubei, H.M.; Zedini, E.; Elafandy, R.T.; Kammoun, A.; Abdallah, M.; Ng, T.K.; Hamdi, M.; Alouini, M.-S.; Ooi, B.S. Simple statistical channel model for weak temperature-induced turbulence in underwater wireless optical communication systems. *Opt. Lett.* **2017**, *42*, 2455–2458. [[CrossRef](#)] [[PubMed](#)]
14. Geldard, C.T.; Thompson, J.; Popoola, W.O. Empirical Study of the Underwater Turbulence Effect on Non-Coherent Light. *IEEE Photon.-Technol. Lett.* **2020**, *32*, 1307–1310. [[CrossRef](#)]
15. Oubei, H.M.; Zedini, E.; Elafandy, R.T.; Kammoun, A.; Ng, T.K.; Alouini, M.-S.; Ooi, B.S. Efficient Weibull channel model for salinity induced turbulent underwater wireless optical communications. In Proceedings of the 2017 Opto-Electronics and Communications Conference (OECC) and Photonics Global Conference (PGC), Singapore, 31 July–4 August 2017; pp. 1–2. [[CrossRef](#)]
16. Zedini, E.; Oubei, H.M.; Kammoun, A.; Hamdi, M.; Ooi, B.S.; Alouini, M.-S. Unified Statistical Channel Model for Turbulence-Induced Fading in Underwater Wireless Optical Communication Systems. *IEEE Trans. Commun.* **2019**, *67*, 2893–2907. [[CrossRef](#)]
17. Jiang, H.; Qiu, H.; He, N.; Zhao, Z.; Popoola, W.; Ahmad, Z.; Rajbhandari, S. LDPC-coded CAP with spatial diversity for UVLC systems over generalized-gamma fading channel. *Sensors* **2020**, *20*, 3378. [[CrossRef](#)]
18. Jamali, M.V.; Akhoundi, F.; Salehi, J.A. Performance characterization of relay-assisted wireless optical CDMA networks in turbulent underwater channel. *IEEE Trans. Wirel. Commun.* **2016**, *15*, 4104–4116. [[CrossRef](#)]
19. Gökçe, M.C.; Baykal, Y. Aperture averaging and BER for Gaussian beam in underwater oceanic turbulence. *Opt. Commun.* **2018**, *410*, 830–835. [[CrossRef](#)]
20. Jamali, M.V.; Nabavi, P.; Salehi, J.A. MIMO underwater visible light communications: Comprehensive channel study, performance analysis, and multiple-symbol detection. *IEEE Trans. Veh. Technol.* **2018**, *67*, 8223–8237. [[CrossRef](#)]
21. Zhu, B.; Cheng, J.; Yan, J.; Wu, L.; Wang, Y.; Wang, J. A New Asymptotic Analysis Technique for Diversity Reception Over Correlated Lognormal Fading Channels. *IEEE Trans. Commun.* **2017**, *66*, 845–861. [[CrossRef](#)]
22. Xu, F.; Khalighi, A.; Caussé, P.; Bourennane, S. Channel coding and time-diversity for optical wireless links. *Opt. Express* **2009**, *17*, 872–887. [[CrossRef](#)]
23. Ghassemlooy, Z.; Popoola, W.; Rajbhandari, S. *Optical Wireless Communications: System and Channel Modelling with MATLAB*; CRC Press: Boca Raton, FL, USA, 2012.
24. Nistazakis, H.E.; Stassinakis, A.N.; Sinanović, S.; Popoola, W.O.; Tombras, G.S. Performance of quadrature amplitude modulation orthogonal frequency division multiplexing-based free space optical links with non-linear clipping effect over gamma-gamma modelled turbulence channels. *Optoelectron. IET* **2017**, *9*, 269–274. [[CrossRef](#)]
25. Jiao, W.; Liu, H.; Yin, J.; Wei, Z.; Luo, A.; Deng, D. Performance of a QAM/FSO communication system employing spatial diversity in weak and saturation turbulence channels. *J. Mod. Opt.* **2019**, *66*, 965–975. [[CrossRef](#)]
26. Chatzidiamentis, N.; Lioumpas, A.; Karagiannidis, G.K.; Arnon, S. Adaptive subcarrier PSK intensity modulation in free space optical systems. *IEEE Trans. Commun.* **2011**, *59*, 1368–1377. [[CrossRef](#)]
27. Khallaf, H.S.; Shalaby, H.M.H.; Balsells, J.M.G.; Sampei, S. Performance analysis of a hybrid QAM-MPPM technique over turbulence-free and gamma-gamma free-space optical channels. *J. Opt. Commun. Netw.* **2017**, *9*, 161–171. [[CrossRef](#)]
28. Yin, C.S.; He, Z.Y.; Deng, S.; Liang, S.; He, N. Investigation on pulse response and the large current optical modulation of high power LEDs. *J. Optoelectron. Laser* **2015**, *26*, 1041–1047.
29. Xu, F.; Khalighi, M.-A.; Bourennane, S. Coded PPM and Multipulse PPM and Iterative Detection for Free-Space Optical Links. *J. Opt. Commun. Netw.* **2009**, *1*, 404–415. [[CrossRef](#)]
30. Wang, P.; Yang, B.; Guo, L.; Shang, T. SER performance analysis of MPPM FSO system with three decision thresholds over exponentiated Weibull fading channels. *Opt. Commun.* **2015**, *354*, 1–8. [[CrossRef](#)]
31. Zhou, D.; Cao, T.; Yang, Y.; Zhang, J.; Wang, P.; Yang, B. Symbol error rate performance analysis of soft-decision decoded MPPM free space optical system over exponentiated Weibull fading channels. *Chin. Opt. Lett.* **2017**, *15*, 50602–50606. [[CrossRef](#)]
32. Bykhovsky, D. Symbol error rate of soft-decision multiple pulse position modulation over turbulent channels. *Appl. Opt.* **2019**, *58*, 1193–1199. [[CrossRef](#)]
33. Peppas, K.P.; Boucouvalas, A.C.; Ghassemlooy, Z. Performance of underwater optical wireless communication with multi-pulse pulse-position modulation receivers and spatial diversity. *IET Optoelectron.* **2017**, *11*, 180–185. [[CrossRef](#)]
34. Jurado-Navas, A.; Serrato, N.G.; Garrido-Balsells, J.M.; Castillo-Vázquez, M. Error probability analysis of OOK and variable weight MPPM coding schemes for underwater optical communication systems affected by salinity turbulence. *OSA Contin.* **2018**, *1*, 1131–1143. [[CrossRef](#)]
35. Hou, J.; Siegel, P.; Milstein, L. Performance analysis and code optimization of low density parity-check codes on Rayleigh fading channels. *IEEE J. Sel. Areas Commun.* **2001**, *19*, 924–934. [[CrossRef](#)]
36. Anguita, J.A.; Djordjevic, I.B.; Neifeld, M.A.; Vasic, B.V. Shannon capacities and error-correction codes for optical atmospheric turbulent channels. *J. Opt. Netw.* **2005**, *4*, 586–601. [[CrossRef](#)]
37. Djordjevic, I.B.; Vasic, B.; Neifeld, M.A. LDPC coded OFDM over the atmospheric turbulence channel. *Opt. Express* **2007**, *15*, 6336–6350. [[CrossRef](#)] [[PubMed](#)]
38. *IEEE Std 802. 16-2009*; IEEE Standard for Local and Metropolitan Area Networks Part 16: Air Interface for Broadband Wireless Access Systems. IEEE: New York, NY, USA, 2009; pp. 1–2080.
39. Yuan, J.; Liu, F.; Ye, W.; Huang, S.; Wang, Y. A new coding scheme of QC-LDPC codes for optical transmission systems. *Optik* **2014**, *125*, 1016–1019. [[CrossRef](#)]

-
40. Islam, M.R.; Han, Y.S. Cooperative MIMO communication at wireless sensor network: An error correcting code approach. *Sensors* **2011**, *11*, 9887–9903. [[CrossRef](#)]
 41. Hamkins, J.; Moision, B. Multipulse Pulse-Position Modulation on Discrete Memoryless Channels. *Interplanet. Netw. Prog. Rep.* **2005**, *42*, 1–13.
 42. Du, J.; Zhou, T.; Chen, W.; Hu, F. Performance Analysis of Underwater Optical Communication Based on LDPC and PPM. *Laser Optoelectron. Prog.* **2016**, *53*, 120605.
 43. Jurado-Navas, A.; Álvarez-Roa, C.; Álvarez-Roa, M.; Castillo-Vázquez, M. Cooperative Terrestrial-Underwater Wireless Optical Links by Using an Amplify-and-Forward Strategy. *Sensors* **2022**, *22*, 2464. [[CrossRef](#)]
 44. Elamassie, M.; Uysal, M. Vertical Underwater Visible Light Communication Links: Channel Modeling and Performance Analysis. *IEEE Trans. Wirel. Commun.* **2020**, *19*, 6948–6959. [[CrossRef](#)]
 45. Popoola, W.O.; Ghassemlooy, Z. BPSK subcarrier intensity modulated free-space optical communications in atmospheric turbulence. *J. Light. Technol.* **2009**, *27*, 967–973. [[CrossRef](#)]